AD-A126 359 GLOBAL SOLUTION PROCEDURES FOR INCOMPRESSIBLE LAMINAR FLOW WITH STRONG PR.. (U) CINCINNATI UNIV OH DEPT OF AEROSPACE ENGINEERING AND APPLIED M.. S G RUBIN ET AL. 1/1

UNCLASSIFIED JAN 83 AFOSR-TR-83-0125 AFOSR-80-0047 F/G 20/4 NL

END

FILMED
-83
DTIC

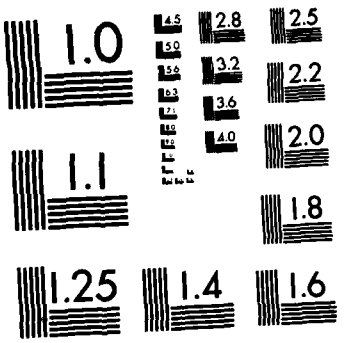

UNCLASSIFIED

SECURITY CLASSIFICATION OF THIS PAGE (When Data Entered)

2

REPORT DOCUMENTATION PAGE		READ INSTRUCTIONS BEFORE COMPLETING FORM
1. REPORT NUMBER AFOSR-TR- 83-0125	2. GOVT ACCESSION NO.	3. RECIPIENT'S CATALOG NUMBER
4. TITLE (and Subtitle) GLOBAL SOLUTION PROCEDURES FOR INCOMPRESSIBLE LAMINAR FLOW WITH STRONG PRESSURE INTERACTION AND SEPARATION		5. TYPE OF REPORT & PERIOD COVERED INTERIM 6. PERFORMING ORG. REPORT NUMBER
7. AUTHOR(s) S G RUBIN D R REDDY		8. CONTRACT OR GRANT NUMBER(s) AFOSR-80-0047
9. PERFORMING ORGANIZATION NAME AND ADDRESS UNIVERSITY OF CINCINNATI DEPT OF AEROSPACE ENGINEERING & APPLIED MECHANICS CINCINNATI, OH 45221		10. PROGRAM ELEMENT, PROJECT, TASK AREA & WORK UNIT NUMBERS 61102F 2307/A1
11. CONTROLLING OFFICE NAME AND ADDRESS AIR FORCE OFFICE OF SCIENTIFIC RESEARCH/NA BOLLING AFB, DC 20332		12. REPORT DATE January 1983 13. NUMBER OF PAGES 10
14. MONITORING AGENCY NAME & ADDRESS(if different from Controlling Office)		15. SECURITY CLASS. (of this report) UNCLASSIFIED 15a. DECLASSIFICATION/DOWNGRADING SCHEDULE

16. DISTRIBUTION STATEMENT (of this Report)

Approved for Public Release; Distribution Unlimited.

17. DISTRIBUTION STATEMENT (of the abstract entered in Block 20, if different from Report)

18. SUPPLEMENTARY NOTES

Proceedings of the 2nd Symposium on Numerical and Physical Methods for Aerodynamic Flows, Long Beach State University, 17-20 January 1983

19. KEY WORDS (Continue on reverse side if necessary and identify by block number)

NUMERICAL METHODS
RELAXATION SOLUTIONS
SEPARATED FLOW
STRONG INTERACTING FLOW
PARABOLIZED NAVIER-STOKES EQUATIONS

20. ABSTRACT (Continue on reverse side if necessary and identify by block number)

Global or relaxation formulations for the reduced form of the Navier-Stokes equations, frequently referred to as parabolized Navier-Stokes (PNS), are presented. Difference procedures and relaxation solutions for the (u,v,p) system are presented. The continuity equation is satisfied exactly at each grid point and a poisson pressure equation is not required explicitly. The development of a second composite (U,ϕ,G) velocity relaxation procedure for the primitive variable equations is also discussed. For the (u,v,p) system, several model problems, e.g., finite flat plate, trough, boattail and airfoil,

DD FORM 1 JAN 73 1473 EDITION OF 1 NOV 65 IS OBSOLETE

UNCLASSIFIED

SECURITY CLASSIFICATION OF THIS PAGE (When Data Entered)

are considered. Strong pressure interaction is evident in each case and axial flow separation occurs for several of the problems. The questions of accuracy, stability, convergence rate, and implied difference forms of the pressure and vorticity equations are addressed.

PRESENTED AT THE 2ND SYMPOSIUM ON NUMERICAL AND PHYSICAL METHODS FOR AERODYNAMIC FLOWS, Long Beach State University, Long Beach, CA, January 17, through January 20, 1983.

GLOBAL SOLUTION PROCEDURES FOR INCOMPRESSIBLE LAMINAR FLOW WITH STRONG PRESSURE INTERACTION AND SEPARATION†

S.G. Rubin and D.R. Reddy
Department of Aerospace Engineering and Applied Mechanics
University of Cincinnati
Cincinnati, Ohio

Abstract

Global or relaxation formulations for the reduced form of the Navier-Stokes equations, frequently referred to as parabolized Navier-Stokes (PNS), are presented. Difference procedures and relaxation solutions for the (u,v,p) system are presented. The continuity equation is satisfied exactly at each grid point and a poisson pressure equation is not required explicitly. The development of a second composite (U,ϕ,G) velocity relaxation procedure for the primitive variable equations is also discussed. For the (u,v,p) system, several model problems, e.g., finite flat plate, trough, boattail and airfoil, are considered. Strong pressure interaction is evident in each case and axial flow separation occurs for several of the problems. The questions of accuracy, stability, convergence rate, and implied difference forms of the pressure and vorticity equations are addressed.

1. Introduction

Conventional methods for the numerical solution of the primitive variable form of the incompressible (elliptic) Navier-Stokes or ("semi-elliptic") parabolized Navier-Stokes (PNS) equations are such that the velocity components, u,v, are determined from the momentum equations, and the pressure p is obtained from the differential poisson equation derived from the momentum equations. The equation of continuity is not evaluated explicitly but is satisfied indirectly through the poisson equation and pressure boundary conditions. Since this procedure differs markedly from most inviscid, boundary layer and triple deck formulations, an alternate development that more closely follows these asymptotic theories is considered here for the evaluation of viscous interacting flows at large Reynolds numbers.

In the present paper, the authors continue the line of thought first presented for the PNS system in references [1-3]. The analysis is developed in greater detail here and in [4, 5]. The questions of global stability of the relaxation procedure, the resulting difference forms of the pressure and vorticity equations, accuracy and rate of convergence, are examined more critically. Comparisons are given with triple deck and interacting boundary layer solutions for trailing edge and trough configurations; solutions are also obtained for boattail and airfoil geometries. The effects of strong pressure interaction and/or flow separation are evident in each of these problems. The majority of the solutions are for laminar flow conditions; however, several results have been obtained with the Cebeci-Smith two layer eddy viscosity closure model.

The objective of the present development is the solution of the PNS system by direct application of the momentum and (first-order) continuity equations. The formulation does not require the second-order differential form of the poisson pressure solver. A global line relaxation procedure is developed for (u,v,p) or a composite [6, 7] (U,ϕ,G) system. For non-separated flows only p or ϕ are stored during the relaxation process. For separated flows, (u,v) or (U) is required only in regions of reversed flows. This significantly reduces computer storage requirements.

2. Governing Equations

We consider here the reduced set of PNS equations (1, 2) written in two-dimensional or axisymmetric body fitted conformal coordinates. The equations in general orthogonal coordinates are given in [3]. As discussed for cartesian coordinates in [2, 3], for incompressible flow a consistent PNS approximation allows for the neglect of all axial (ξ) diffusion terms as well as all diffusion effects in the normal (η) momentum equation. Normal diffusion can be included in the η-momentum equation; however, for consistency these terms have generally been neglected. Numerical tests with and without these terms have confirmed the validity of this approximation for several of the problems considered herein.

(i) (u,v,p):

continuity

$$(hh_3u)_\xi + (hh_3v)_\eta = 0 \tag{1a}$$

ξ-momentum

$$(hh_3u^2)_\xi + (h^2uv)_\eta + uvh_3h_\eta - v^2h_3h_\xi = -hh_3p_\xi + V\cdot T/R_e \tag{1b}$$

where
$$V\cdot T = [h_3(hu)_\eta/h^2]_\eta \tag{1c}$$

η-momentum

$$hh_3p_\eta = -(hh_3uv)_\xi - (hh_3v^2)_\eta - uvh_\xi + u^2h_3h_\eta \tag{1d}$$

The cartesian coordinates $\xi = \xi(x,y)$, $\eta = \eta(x,y)$ are related to the (x,y) physical coordinates through the transformation $\sigma = f(z)$ or $z = F(\sigma)$ where $\sigma = \xi+i\eta$ and $z = x+iy$. The metric h is defined by

† This research was supported by the Air Force Office of Scientific Research under Grant No. AFOSR 80-0047.

$$h = |f'(z)| = (x_\xi^2 + y_\xi^2)^{1/2} = (x_\eta^2 + y_\eta^2)^{1/2}$$

The metric $h_3 = y^\epsilon$, where $\epsilon = 0$ for two-dimensions and $\epsilon = 1$ for axisymmetry. The metric h and all derivatives are evaluated with second-order difference formulas. In the axial and normal momentum equations (1b, 1c), the metric h and derivatives of h are assumed to be at most of order one. For geometries with larger curvature the complete expression for $\nabla\cdot T$ may be required in (1b) and the viscous effects in (1d) may become important. The full Navier-Stokes equations or a more appropriate non-conformal coordinate mapping may then be required, see [6, 7].

(ii) (U,ϕ,G):

In the composite velocity development described in [6, 7], an "inviscid" pseudo-potential ϕ, "viscous" velocity U and "inviscid" Bernoulli pressure G, replace (u,v,p), i.e.,

$$u = U(1 + \phi_\xi)/h = U\, u_e$$

$$v = \phi_\eta/h$$

$$G = p/\rho + (u_e^2 + v^2)/2 - G_\infty$$

The equations become

continuity

$$(h_3 U\phi_\xi)_\xi + (h_3\phi_\eta)_\eta + (h_3 U)_\xi = 0 \qquad (2a)$$

ξ-momentum

$$u_t + \{[hh_3\, u_e^2(U^2-U)]_\xi + [hh_3 u_e v(U-1)]_\eta\}/h^2h_3$$

$$+ u_e v h_\eta (U-1)/h^2 + u_e u_{e\xi}\,(U-1)/h$$

$$= - G_\xi/h + \nabla\cdot T/R_e \qquad (2b)$$

η-momentum

$$G_\eta = - (U-1)\,\{(u_e^2/2)_\eta - u_e^2 U h_\eta/h\} \qquad (2c)$$

This multiplicative composite velocity development is patterned after matched asymptotic viscous-inviscid flow theory. For inviscid irrotational flows, $U \equiv 1$; (2a) then reduces to the potential equation and (2b,c) lead to the Bernoulli equation, $G = 0$. For boundary layer problems, u_e, $u_{e\xi}$ (or ϕ_ξ, $\phi_{\xi\xi}$) and G are specified with boundary layer edge conditions and (2a,b) combine to determine (U,v). Interacting boundary layer theory combines elements of both limits, so that (2a,b) form a coupled system for (U,ϕ), with G prescribed. The equations (1) or (2) contain all the terms appearing in each layer of the triple deck structure [3].

The present investigation concentrates on the (u,v,p) formulation described by equations (1). Composite solutions have already been discussed for the full Navier-Stokes equations in [6, 7]. Analysis of the PNS equations with the composite system is in progress and results with this formulation shall be presented in a future paper.

3. Difference Equations

In the previous analyses [1-3], it was shown that if the system (1) was forward marched in the boundary layer sense, i.e., backward differences are applied for all ξ derivatives in non-separated regions, the elliptic pressure interaction would not be properly represented and therefore the exponentially growing Lighthill departure solutions would appear for step sizes $\Delta\xi < (\Delta\xi)_{min}$. For cartesian coordinates, from [2, 3], we find that $(\Delta\xi)_{min} = \frac{2}{\pi} y_M$, where y_M is the location of the outer boundary $y = y_M$. Only for $y_M \ll 1$ are accurate solutions possible with forward marching.

If global relaxation or multiple sweep marching is used, i.e., all ξ derivatives of velocities are backward differenced in non-separated regions, but some form of forward differencing is applied for p_ξ in (1a), the elliptic pressure interaction is recovered and the departure free limit $\Delta\xi > (\Delta\xi)_{min}$ is removed. Solutions can then be obtained for $\Delta\xi \to 0$, see [2, 3]; the numerical procedure is consistent and any desired degree of accuracy can be specified. Finally, in order to circumvent the pressure singularity at separation, the p_ξ term must also allow for a local as well as a spatial interaction. For example, central differencing fails in this regard and, as discussed in [2, 3], is unstable globally. Forward differencing of p_ξ satisfies all constraints and moreover is consistent with the eigenvalue analysis of Vigneron et al. [9] which shows that for incompressible flow ($M \to 0$), there should not be any forward marched component of the p_ξ term; i.e., $\omega = 0$ in his analysis. Forward differencing and global relaxation was first applied successfully in [1-3] for several model incompressible flow problems. The extension to compressible flows is discussed for a conical geometry in [2] and for flows with axial flow separation and strong pressure interaction in [10]. More detailed discussion and results are given in [3, 4].

The difference scheme used in [1-3] was developed from the following discrete grid:

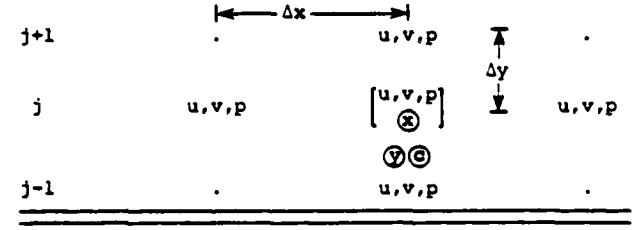

Figure 1: Difference Grid I.

The continuity, x and y momentum equations are centered at ⓒ, ⓧ and Ⓨ, respectively and the difference equations given for a uniform mesh in cartesian coordinates are as follows.

continuity, centered at $(i,j-\frac{1}{2})$:

$$\frac{u_{i,j}-u_{i-1,j}+u_{i,j-1}-u_{i-1,j-1}}{2\Delta x}+\frac{v_{i,j}-v_{i,j-1}}{\Delta y}=0 \qquad (3a)$$

x-momentum, centered at (i,j):

$$u_{i,j}\left(\frac{u_{i,j}-u_{i-1,j}}{\Delta x}\right)+v_{i,j}\left(\frac{u_{i,j+1}-u_{i,j-1}}{2\Delta y}\right)+\frac{p^{n-1}_{i+1}-p_i}{\Delta x}=\frac{1}{Re}\left(\frac{u_{i,j+1}-2u_{i,j}+u_{i,j-1}}{\Delta y^2}\right) \qquad (3b)$$

y-momentum, centered at $(i,j-\frac{1}{2})$:

$$-\frac{p_{i,j}-p_{i,j-1}}{\Delta y}=\left(\frac{u_{i,j}+u_{i,j-1}}{2}\right)\left(\frac{v_{i,j}-v_{i-1,j}+v_{i,j-1}-v_{i-1,j-1}}{2\Delta x}\right)+\left(\frac{v_{i,j}+v_{i,j-1}}{2}\right)\left(\frac{v_{i,j}-v_{i,j-1}}{\Delta y}\right) \qquad (3c)$$

The equations are shown here in non-conservative form as this simplifies the subsequent discussion of the linear system. In fact, for most calculations conservative equations were considered. All quantities are evaluated at the n^{th} iteration level except p^{n-1}_{i+1}, which is evaluated at the previous iteration. For separated flows the convective terms are upwinded and u^{n-1}_{i+1}, v^{n-1}_{i+1} terms are also required at level n-1. The difference equations (3) are first-order accurate, i.e., $O(\Delta x, \Delta y^2)$.

An alternate and more accurate derivation of the equations and interpretation of "forward" differencing for p_{i+1} is given below for cartesian coordinates. This system was considered initially for inviscid flows [4] and resembles a slightly different development proposed by Israeli [8]. Consider the staggered difference grid as shown:

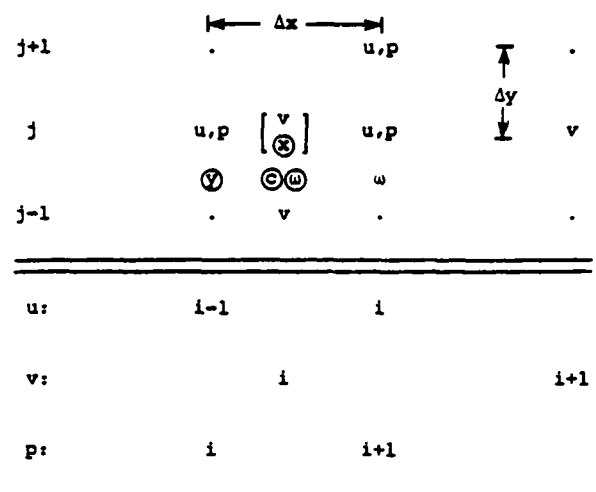

Figure 2: Difference Grid II

The appropriate difference equations, also shown in non-conservative form, are now centered at somewhat different ⓒ, ⓧ, Ⓨ locations.

continuity, centered at ⓒ is the same as (3a):

$$\frac{u_{i,j}-u_{i-1,j}+u_{i,j-1}-u_{i-1,j-1}}{2\Delta x}+\frac{v_{i,j}-v_{i,j-1}}{\Delta y}=0 \qquad (4a)$$

x-momentum, centered at ⓧ:

$$\left(\frac{u_{i,j}+u_{i-1,j}}{2}\right)\left(\frac{u_{i,j}-u_{i-1,j}}{\Delta x}\right)+v_{i,j}\left(\frac{u_{i,j+1}-u_{i,j-1}+u_{i-1,j+1}-u_{i-1,j-1}}{4\Delta y}\right)+\frac{p^{n-1}_{i+1,j}-p_{i,j}}{\Delta x}=\frac{1}{Re}\left(\frac{u_{i,j+1}-2u_{i,j}+u_{i,j-1}+u_{i-1,j+1}-2u_{i-1,j}+u_{i-1,j-1}}{2\Delta y^2}\right) \qquad (4b)$$

y-momentum, centered at Ⓨ:

$$-\frac{p_{i,j}-p_{i,j-1}}{\Delta y}=\left(\frac{u_{i-1,j}+u_{i-1,j-1}}{2}\right)\left(\frac{v_{i,j}-v_{i-1,j}+v_{i,j-1}-v_{i-1,j-1}}{2\Delta x}\right)+\frac{1}{4}\left(v_{i,j}+v_{i-1,j}+v_{i,j-1}+v_{i-1,j-1}\right)\times\left(\frac{v_{i,j}-v_{i,j-1}+v_{i-1,j}-v_{i-1,j-1}}{2\Delta y}\right) \qquad (4c)$$

In this formulation full second-order accuracy is achieved. The primary modification of the system (3) is the averaging of the y-derivative terms in the momentum equations. The unknown pressure p_i is also shifted one point to the left of that given by the formulation (3). This interpretation is more accurate and is consistent with the character of the interactive solutions as will be seen for the trailing edge problem to be discussed in a following section.

A third system of equations, which also provides second-order accuracy has been proposed by Israeli [8]. The staggered u,v grid is then of the form:

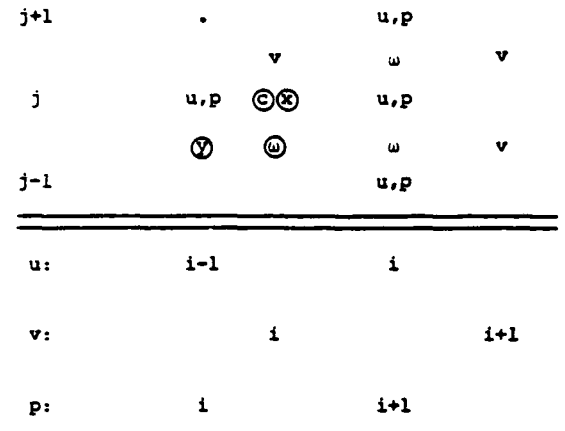

Figure 3: Difference Grid III.

The equations are only slightly modified from those of (4); however, the y boundary condition for v must be treated somewhat differently.

(i) Definition of vorticity and vorticity transport equation:

If the nonlinear coefficients u and v are assumed constant and the pressure is eliminated from (4a,4b), the following difference equation is obtained, in the inviscid limit, for the vorticity transport [4]:

$$u\left(\frac{\omega_{i,j}-\omega_{i-1,j}}{\Delta x}\right) + v\left(\frac{\omega_{i,j+1}-\omega_{i,j-1}+\omega_{i-1,j+1}-\omega_{i-1,j-1}}{4\Delta y}\right) = O(\Delta x^2,\ \Delta y^2) \qquad (5a)$$

where

$$\omega_{i,j} = \frac{v_{i+1,j}-v_{i,j}+v_{i+1,j-1}-v_{i,j-1}}{2\Delta x} - \frac{u_{i,j}-u_{i,j-1}}{\Delta y} \qquad (5b)$$

This corresponds to defining ω at the location ω shown in Figure 2 and centering (5a) at location ⓦ. Both expressions (5a) and (5b) are second-order accurate. The difference equation obtained by replacing $\omega_{i,j}$ terms in (5a) with the formula (5b) is exactly that resulting from the elimination of the pressure in (4a) and (4b) except for the vv_{xy} term in $v\omega_y$; however, with the definition (5b) the error in this expression is $O(\Delta x^2, \Delta y^2)$, so that second-order accuracy is retained in the difference approximation of the vorticity transport equation, see [4]. Similar results can be obtained with the scheme proposed by Israeli in Figure 3.

If (5b) and the continuity equation (3a) are combined to eliminate either u or v terms, for $\omega = 0$ we recover a nine-point second-order accurate difference formula for either $\nabla^2 u = 0$ or $\nabla^2 v = 0$. In fact, inviscid irrotational flows can be solved numerically with (5b) and (3a), in lieu of the potential equation $\nabla^2\phi = 0$. This is a result of backward differencing of u_x in the continuity equation and, as seen in (5b), forward differencing of v_x in the definition of vorticity. One boundary condition is satisfied for u (left boundary) and one for v (right boundary). This is a direct result of the differencing procedure applied for the u,v,p primitive variable system; i.e., backward differences for velocities (in non-separated regions) and "forward" pressure differences as interpreted in Figure 1 (first-order accuracy) or Figure 2 or 3 (second-order accuracy). Further details of this analysis are given in [4].

(ii) Difference equation for pressure:

In a similar manner, the effective poisson difference equation for the pressure can be obtained by $(\text{x-mom})_{i,j} - (\text{x-mom})_{i-1,j} + (\text{y-mom})_{i,j+1} - (\text{y-mom})_{i,j} = 0$. This equation is of the form (see [4] for derivation)

$$\sigma p_{i,j+1} - [(p^{n-1}_{i,j} + p_{i,j}) + 2\sigma(p_{i,j})] + \sigma p_{i,j-1} + p^{n-1}_{i+1,j} + p_{i-1,j} = f_{i,j}(u,v) \qquad (6a)$$

where $\sigma = (\Delta x/\Delta y)^2$.

In order to recover the more conventional line relaxation form of the difference equation, Israeli [5] has shown that if a source term $S_{i,j}$ is introduced in the x-momentum equation (3b or 4b), we obtain

$$\sigma p_{i,j+1} - 2(1+\sigma)p_{i,j} + \sigma p_{i,j-1} + p^{n-1}_{i+1,j} + p_{i-1,j} = \bar{f}_{i,j}(u,v) \qquad (6b)$$

where $S_{i,j} = S_{i-1,j} - p^{n-1}_{i,j} + p_{i,j}$.

This is equivalent to introducing an iterative "time" derivative into the relaxation process. Israeli [5] has also introduced an overrelaxation parameter ϵ as a mechanism to improve convergence rate. Our experience has not led to a marked improvement in convergence for the nonlinear system (4) with overrelaxation. Therefore, all solutions depicted herein are for the first-order system (5a) or the second-order system (5b) with $\epsilon = 1$. Multi-grid procedures have been applied

for convergence acceleration when fine meshes are required, see [4].

It should be reiterated here that although a poisson-like relaxation scheme can be inferred, boundary conditions are prescribed for p only at the outer (y) boundary and downstream (x) boundary; also, the pointwise continuity equation is satisfied exactly. As noted in the introduction, this is in sharp contrast with conventional solution procedures that use the poisson form of the pressure equation with full Neumann boundary conditions and only indirectly satisfy the pointwise continuity equation.

4. Consistency and Convergence

In order to complete the analysis of the relaxation technique discussed herein, two questions are posed. Does the prescribed differencing procedure capture the elliptic pressure interaction in each sweep of the iteration cycle, and what are the convergence properties of the global relaxation process. The first question has been addressed in [1-3] and as discussed in section 3, the departure effect is circumvented and the elliptic interaction is captured with the forward pressure differencing of (3b) or (4b). As shown in [4], the introduction of the source terms $S_{i,j}$ provides increased numerical damping and enhances the stability properties in each marching step.

The second question is considered in detail in reference [4]. The primary conclusions are presented here. Although the forward pressure differencing eliminates the inconsistency found with single sweep procedures, so that $\Delta\xi$ can be made arbitrarily small, the departure limit $\Delta x > 2y_M/\pi$ appears indirectly as a factor affecting convergence of the global relaxation procedure.

It can be shown from a linear global stability analysis that central differencing of p_x is unstable [2-4], but with forward differencing of p_x, as in (3b), the iteration technique is unconditionally stable. The maximum eigenvalue is given [3, 4] as

$$\lambda = 1 - c_1 \pi^2 \left(\frac{\Delta x}{y_M}\right)^4 N_x^2$$

or

$$\lambda = 1 - c_1 \left(\frac{\pi \Delta x}{y_M}\right)^2 \left(\frac{x_M}{y_M}\right)^2$$

where c_1 is a constant of order one, y_M is the outer y boundary, x_M is the outer x boundary, and N_x is the number of x grid points; i.e., $N_x = x_M/\Delta x$. Therefore for $\frac{\pi \Delta x}{y_M} \ll 1$ or $\Delta x \ll \frac{y_M}{\pi}$, $\lambda \to 1$ and the convergence rate will deteriorate. For $\left(\frac{\Delta x}{y_M}\right) \ll 1$ and N_x fixed, convergence is very slow as $\lambda = 1 - \left(\frac{\Delta x}{y_M}\right)^4$. Although the departure limit $\frac{\pi \Delta x}{2y_M} > 1$ is no longer a stability limitation, the condition $\frac{\pi \Delta x}{y_M} \ll 1$ is a convergence limit. For coarser grids, e.g., $\frac{\Delta x}{y_M} > \frac{1}{20}$, convergence is quite rapid. For finer grids, SOR or multigrid acceleration has been considered [4, 5].

The outer pressure boundary condition must be prescribed at a location beyond the extent of the interaction zone of influence, e.g., triple deck. The pressure boundary condition can be fixed during each sweep of the global procedure. This value will remain unchanged if the outer boundary is sufficiently far from, and unaffected by, the viscous interaction; alternatively, the pressure boundary condition can be updated prior to each sweep in order to account for viscous displacement effects. In conformal body fitted or streamline coordinates, this should be unnecessary. Unlike interactive boundary layer theory, where the outer pressure boundary value requires a local interactive treatment in order to circumvent the separation point singularity, a fixed outer pressure condition is acceptable with the PNS formulation. The normal momentum equation reflects the outer inviscid or interactive behavior and the separation singularity is automatically suppressed.

To summarize, if p_x is treated explicitly or central differenced, the global procedure is unstable; if p_x is backward differenced, departure solutions appear for $\Delta x \to 0$. With "forward" differencing all iterative procedures are stable and the global marching problem is well-posed.

5. Boundary Conditions

For the finite-difference grids of Figures 1 or 2 the appropriate boundary conditions are specified as follows in the transformed body fitted coordinate system:

At a surface $y = 0$ ($j = 0$), the velocities $u = v = 0$; at a symmetry line $y = 0$ ($j = 0$), the velocities satisfy $u_y = v = 0$.

At the outer boundary $y = y_M$ ($j = M$), where y_M lies outside of the extent of the interaction zone, e.g., triple deck, $p = p_\infty$, $u = u_\infty$ and a boundary condition on v is not required.

At the inflow boundary $x = 0$ ($i = 1$), $u = u(0,y)$, and $v_x(0,y) = 0$. For inviscid regions, where $u = u_\infty$, $v_x = 0$ is a zero vorticity condition and for viscous regions $v_x = 0$ is equivalent to a boundary layer approximation. The velocity v should not be specified at the inflow. This leads to inviscid vorticity production and has a destabilizing effect on the global iteration procedure. The flow pressure is not prescribed and with the formulation of Figure 2 is unknown and a result of the calculation procedure.

Finally, the only boundary condition required at the outflow is the pressure or equivalent pressure gradient. This of course reflects the elliptic pressure interaction.

6. Solutions

Five model problems have served as test cases for the global PNS formulation described herein. For each geometry there is a region of strong pressure interaction and in several cases axial flow separation occurs. The test problems include (1) the trailing edge of a flat plate, (2) the Carter-Wornom [12] trough, (3) a boattail configuration, (4) a NACA 0012 airfoil at zero incidence (laminar), and (5) the NACA 0012 airfoil at zero incidence (turbulent).

(i) Trailing Edge

Solutions for the trailing edge geometry are given in figures (4a,4b). The agreement with the interacting boundary layer results of [11] are quite good. The finest grid includes (161 x 121) mesh points for (x,y), respectively. The coarsest grid was (41 x 121) and full convergence required only several global iterations. If the calculation was run on the finest grid alone, convergence was still not achieved after several hundred iterations. With a multigrid technique [4], full convergence to $O(10^{-4})$ for the maximum error in successive iterations was achieved in approximately ten to fifteen global iterations. The outer boundary y_M was chosen to lie outside the triple deck extent. If y_M violated this condition, the calculation diverged. The calculation was relatively insensitive to y_M when this condition was satisfied.

The solutions for pressure and skin friction, both defined with triple deck normalization [11] are shown for $Re = 10^5$. It is significant that the skin friction (velocity profile) is relatively insensitive to the grid and appears to be quite acceptable even on some of the coarser meshes. On the other hand, the pressure is extremely grid sensitive and requires the finest mesh in order to accurately represent the triple deck interaction. With the difference grid of Figure 1, the minimum pressure occurs one grid point downstream of the trailing edge. With the grid of Figure 2 this pressure value is correctly obtained at the trailing edge.

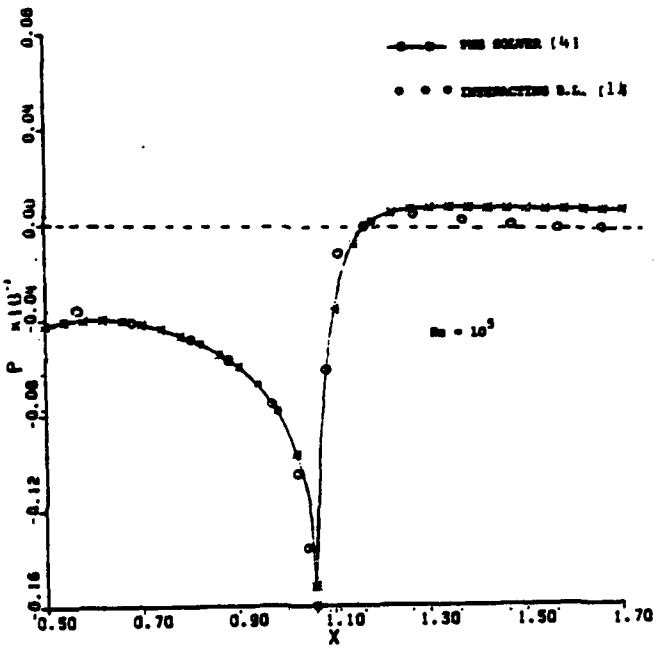

Figure 4a. Trailing Edge Pressure Distributions PNS Solver.

(ii) Trough

The solutions for the trough geometry $[y_b(x) = \varepsilon \text{ sech } 4(x - 2.5)]$, $(0 \leq x \leq \infty)$ are shown in Figures (5a, 5b). Values of $\varepsilon = -0.015$ [3, 4] and $\varepsilon = -0.03$ were considered. Only the latter results are presented here. Solutions were obtained for Reynolds numbers up to $Re = 3.6 \times 10^5$. Again, the agreement with the interacting boundary layer solutions is quite good. The insensitivity of C_f and the sensitivity of p to the grid is also evident for this example. As the Reynolds number was increased, more smoothing was required on the coarser grids in order to achieve convergence to the prescribed tolerance. The outer undisturbed pressure boundary condition was held fixed at $y = y_M$ throughout the computation. There were no difficulties at separation or reattachment points. As with the trailing edge problem, full convergence with the multi-grid iteration procedure was achieved in ten to fifteen global iterations. For the finest grid (241 x 121) mesh points were evaluated.

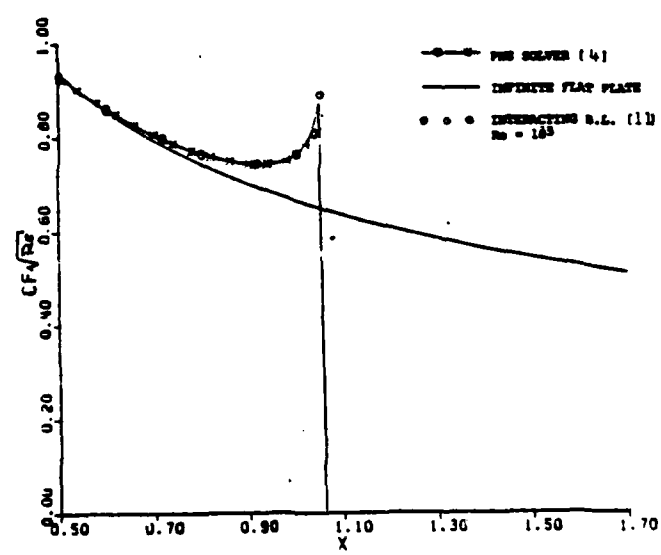

Figure 4b. Trailing Edge Skin Friction Solutions PNS Solver.

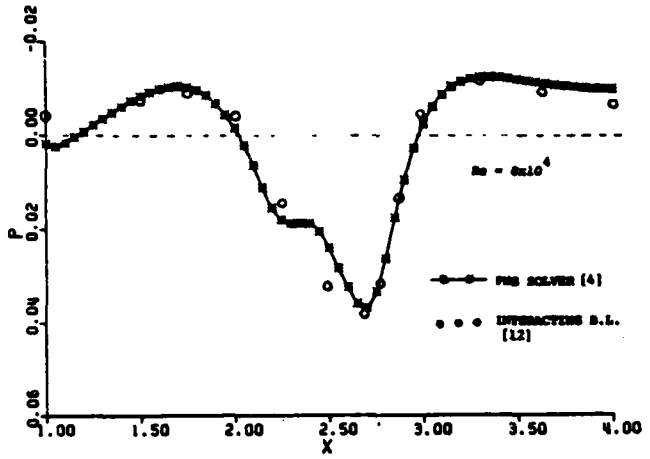

Figure 5a. Trough Skin-Friction Solutions PNS Solver: $\varepsilon = -0.03$.

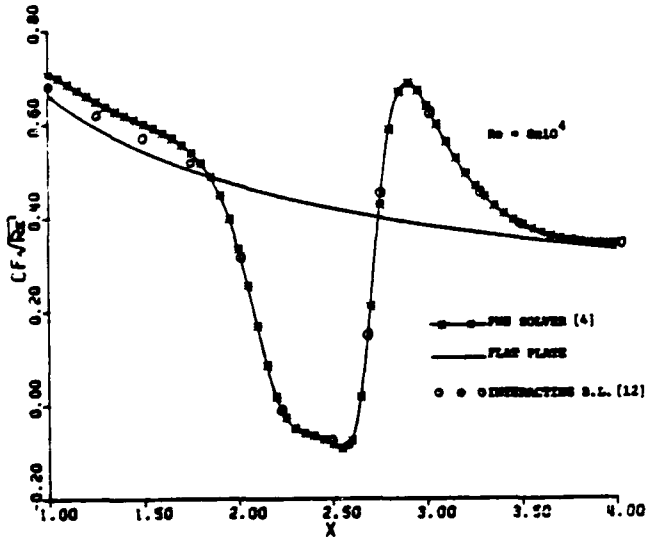

Fig. 5b. Trough Pressure Solutions PNS Solver: $\varepsilon = -0.03$.

(iii) Boattail

Laminar flow solutions for the boattail geometry of Figure 6 are shown in Figures (7a, 7b, 7c). The grid is generated with the Schwarz-Christoffel mapping routine of Davis [13]. These results are in good agreement with full Navier-Stokes solutions obtained with the composite (u,ϕ,G) equations as reported in [3, 7]. For Re = 6000, based on maximum radius, with a juncture angle of 12 degrees a sizable separation bubble is obtained. All velocities are stored in the recirculation region. The relaxation process is slower than for the trailing edge or trough geometries; however, convergence to 10^{-4} for the maximum error in pressure is obtained in approximately 35 iterations. As the Reynolds number or corner angle is increased, the rate of convergence decreases and the multigrid procedure also deteriorates. Further analysis of this behavior is required. Some improvement has been observed with the source correction of (5b).

Solutions have also been obtained for turbulent flow conditions. The Cebeci-Smith two layer viscosity model has been applied to close the system. Although this may not be an accurate approximation in the recirculation region, it does serve to give a qualitative picture of the flow. A Reynolds number of Re = 5 x 10^5 based on maximum body radius has been specified. The effective turbulent Reynolds number is of course much lower and the separation region is considerably smaller than that obtained for the laminar flow at Re = 6000. These results are discussed in greater detail and figures are presented in [4].

(iv) Airfoils: laminar and turbulent

The flow over NACA 0012 and 12% thick Joukowski airfoils has been evaluated with global PNS relaxation. Analytic or conformal mapping [13] is used to generate the requisite metric functions for the system (1), Figure 8. Solutions have been obtained for fully laminar conditions for Re = 2000 to 7500. Recirculation is evident for the Joukowski airfoils for Re > 2000. For the NACA 0012 configuration, separation is not evident for Re $\leq$ 5000. Typical laminar solutions are shown in Figures (9a, 9b). The laminar stagnation point results are also in close agreement with the familiar Navier-Stokes (boundary layer) values [4].

Triple deck analyses have recently been presented for separation on cusped and sharp trailing edge airfoils [14, 15]. Estimates of incipient separation as a function of Re are in qualitative agreement with the present numerical solutions, and the flow behavior near the wedge-like trailing edge is also reasonable, see Figure 10. Further comparisons are given in [4].

Finally, for Re = 5 x 10^5, transition to turbulent flow conditions is assumed at x/c = 0.32. The two layer eddy viscosity model should be representative of the turbulent flow behavior as separation does not occur even for this very large value of Re [16]. Comparisons with experimental results and earlier calculations [16] are quite reasonable, see reference [4].

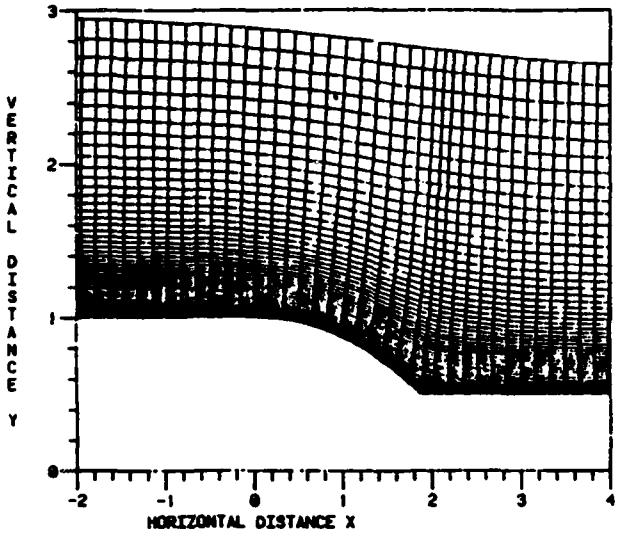

Figure 6. Boattail (BETAC = 15 Deg) Grid Near the Corner.

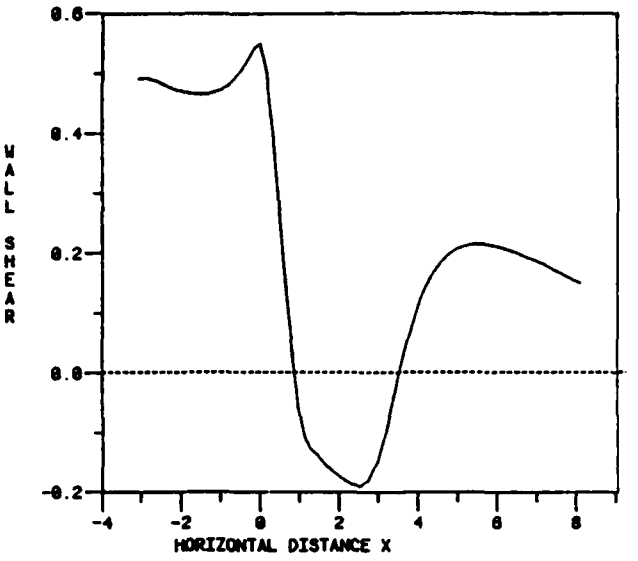

Figure 7b. Boattail (BETAC = 15 Deg) Laminar Flow Re = 1000.

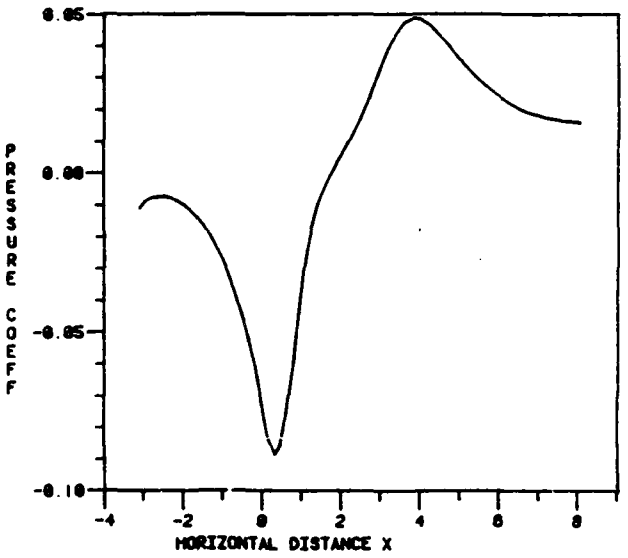

Figure 7a. Boattail (BETAC = 15 Deg) Laminar Flow Re = 1000.

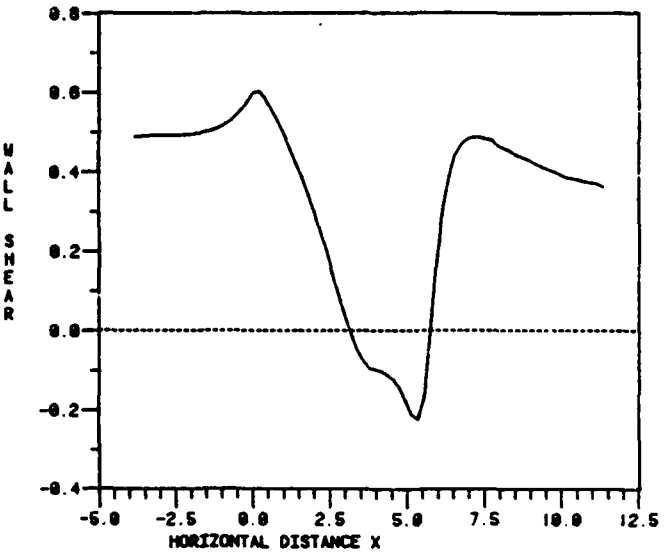

Figure 7c. Boattail (BETAC = 6 Deg) Laminar Flow Re = 6000.

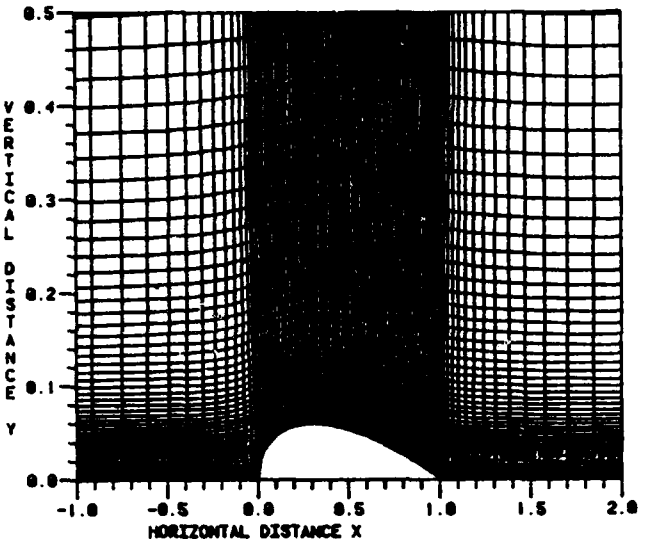

Figure 8. NACA 0012 Airfoil Grid Close to the Body.

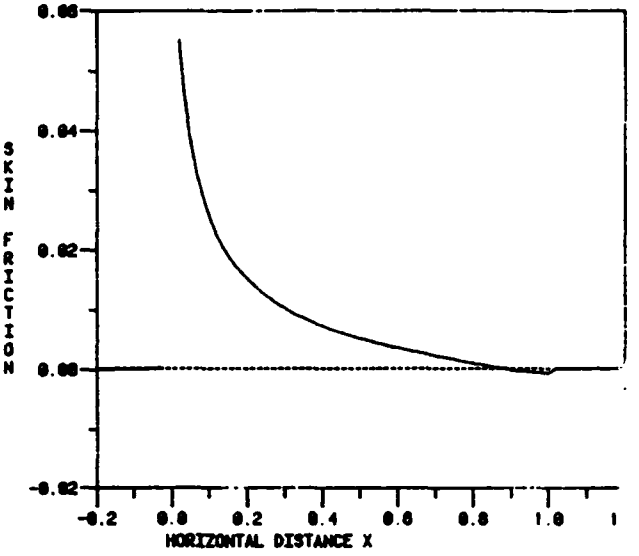

Figure 9b. NACA 0012 Airfoil Laminar Flow (Re = 12,500).

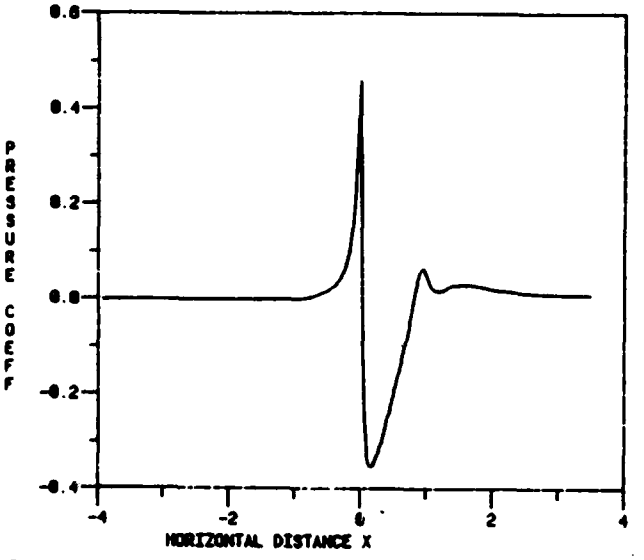

Figure 9a. NACA 0012 Airfoil Laminar Flow (Re = 12,500).

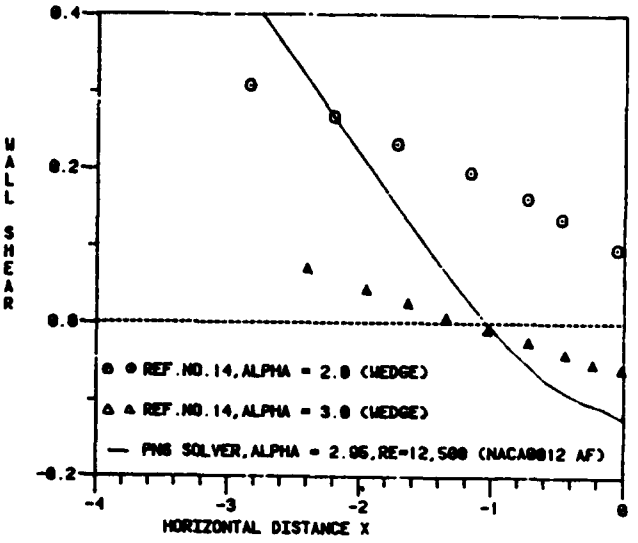

Figure 10. Trailing Edge Results in Triple Deck Scalings.

7. Summary

A global or relaxation procedure for the PNS system of equations has been developed. First and second-order accurate formulations have been presented. In the latter case, a staggered grid is considered and the unknown pressure is evaluated one grid point upstream of the velocity. In the former case, a forward pressure difference is implied. The effective difference forms of the vorticity transport and poisson pressure equations have been derived and results of global stability and convergence analyses have been reported.

Solutions have been obtained for laminar and turbulent flows where strong pressure interaction and/or axial flow separation occurs. The full elliptic pressure interaction is accurately evaluated and with the local pressure interaction there is no separation singularity. Procedures for increasing convergence rates have been examined, e.g., multi-grid; however, further analysis is still necessary, see [4].

Significantly, the differential form of the poisson pressure equation is not required explicitly and the local continuity equation is satisfied exactly at all points.

References

1. Rubin, S.G. and Lin, A. (1980), "Marching with the PNS Equations," Israel J. of Technology, 18, pp. 21-31.

2. Rubin, S.G. (1981), "A Review of Marching Procedures for PNS Equations," 1st Symposium on Numerical and Physical Aspects of Aerodynamic Flows, Long Beach, CA, Springer-Verlag.

3. Rubin, S.G. (1982), "Incompressible Navier-Stokes and PNS Solution Procedures and Computational Techniques," VKI Lecture Notes, Brussels, Belgium; also, to appear in part, in "Recent Advances in Numerical Methods for Fluids," Pineridge Press, 1983.

4. Rubin, S.G. and Reddy, D.R. (1983), "Relaxation Analysis for the PNS Equations," in preparation.

5. Israeli, M. and Lin, A. (1982), "Numerical Solution and Boundary Conditions for Boundary Layer Like Flows," 8th ICNMFD, Aachen, West Germany, Springer-Verlag.

6. Khosla, P.K. and Rubin, S.G. (1982), "A Composite Velocity Procedure for the Compressible Navier-Stokes Equations," AIAA Paper No. 82-0099.

7. Rubin, S.G. and Khosla, P.K. (1982), "A Composite Velocity Procedure for the Incompressible Navier-Stokes Equations," 8th ICNMFD, Aachen, West Germany, Springer-Verlag.

8. Israeli, M. (1982), Private Communication.

9. Vigneron, Y. et al. (1978), "Calculation of Supersonic Viscous Flow Over Delta Wings with Sharp Supersonic Leading Edges," AIAA Paper No. 78-1137.

10. Khosla, P.K. and Lai, H. (1983), "Global PNS Solutions for Subsonic Strong Interaction Flows," submitted for 6th AIAA CFD Conference, Danvers, Mass.

11. Davis, R.T. and Werle, M. (1981), "Progress on Interacting Boundary Layer Calculations at High Reynolds Numbers," 1st Symposium on Numerical and Physical Aspects of Aerodynamic Flows, Long Beach, CA, Springer-Verlag.

12. Carter, J. and Wornom, S. (1975), "Solutions for Incompressible Separated Boundary Layers Including Viscous-Inviscid Interaction," NASA SP-347.

13. Davis, R.T. (1980), "Numerical Methods for Coordinate Generation Based on a Schwarz-Christoffel Mapping Technique," VKI Lecture Notes, Brussels, Belgium, Hemisphere Press.

14. Smith, F.T. and Merkin, J.H. (1982), "Triple-Deck Solutions for Subsonic Flow Past Humps, Steps, Concave or Convex Corners and Wedged Trailing Edges," Computers and Fluids, 10, pp. 7-25.

15. Cheng, H.K. and Smith, F.T. (1982), "The Influence of Airfoil Thickness and Reynolds Number on Separation," ZAMP, 33, pp. 151-180.

16. Von Doenhoff, A.E. (1940), "Investigation of the Boundary Layer About a Symmetrical Airfoil in a Wind Tunnel of Low Turbulence," NACA Wartime Report L-507.

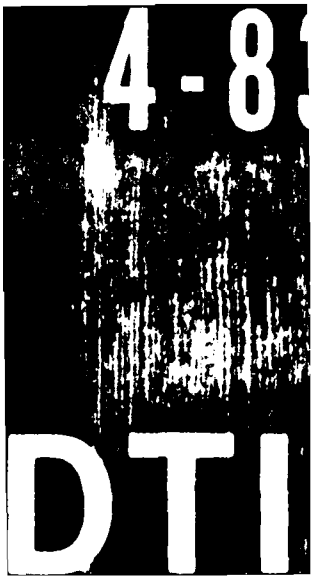
4-8
DTI